

Selective Oxidation of Alcohols in Gas Phase Using Light-Activated Titanium Dioxide

Unnikrishnan R. Pillai and Endalkachew Sahle–Demessie¹

National Risk Management Research Laboratory, Sustainable Technology Division, MS-443, U.S. Environmental Protection Agency, 26 W, Martin Luther King Drive, Cincinnati, Ohio 45268

Received March 29, 2002; revised July 30, 2002; accepted August 6, 2002

Selective oxidation of various primary and secondary alcohols was studied in a gas-phase photochemical reactor using immobilized TiO₂ catalyst. An annular photoreactor was used at 463 K with an average contact time of 32 s. The system was found to be specifically suited for the selective oxidation of primary and secondary aliphatic alcohols to their corresponding carbonyl compounds. Benzylic alcohols gave higher conversions, however, with more secondary reaction products. The reaction mechanism for various products formed is explained. The effects of different reaction parameters, such as O₂/alcohol ratio, water vapor, UV light, and contact time, were studied. The presence of oxygen was found to be critical for the photooxidation. Water vapor in the feed was also found to be helpful in the reaction, although it was not as critical as in hydrocarbon oxidation, where it was necessary for hydroxylating the catalyst surface and sustaining its activity. In alcohol oxidation, surface hydroxylation could be partially provided by the hydroxyl groups of the alcohol itself. Catalyst deactivation was also observed and is attributed to the surface accumulation of reaction products. However, the catalyst regained its original activity after regeneration by calcination in air for 3 h at 723 K. © 2002 Elsevier Science (USA)

Key Words: photocatalytic oxidation; immobilized TiO₂; annular reactor; UV light; alcohol oxidation; carbonyl compounds; catalyst deactivation.

INTRODUCTION

Selective catalytic oxidation of alcohols to carbonyls is one of the most important chemical transformations in industrial chemistry. Carbonyl compounds such as ketones and aldehydes are the precursors for many drugs, vitamins, and fragrances and are also important intermediates for many complex syntheses (1, 2). Most of these reactions, however, use toxic, corrosive, and expensive oxidants, stringent conditions such as high pressure or temperature, and strong mineral acids (3, 4). For example, alcohol oxidation is traditionally carried out in liquid phase by stoichiometric oxidants such as toxic and expensive chromium(VI) and

manganese complexes, which produce a lot of heavy metal waste (1–3). In addition, these reactions are often carried out in environmentally unfriendly organic solvents. Hence replacing them with heterogeneous catalytic oxidation using clean and atom-efficient oxidants such as molecular O₂ and H₂O₂ is a definite need, as well as an important goal of the “green chemistry” concept.

Despite the increasing demand for more-efficient catalytic processes, few efficient catalytic oxidations have been reported for the oxidation of alcohols to carbonyl compounds. Most of these reports use the Mukaiyama route, where O₂ is used in the presence of at least a stoichiometric amount of a reactive aldehyde, which would form the peracid as the actual oxidizing agent (5–7). However, there have also been a few interesting reports which employ aerobic oxidation of alcohols that use copper (8–11), palladium (12, 13), and ruthenium compounds (14–19). Some of these methods are limited to benzylic alcohols and require two equivalents of the catalyst per equivalent of the alcohol (8–10). Marko *et al.* used a copper complex catalyst to oxidize a variety of alcohols, but the method works best in toluene and in the presence of a base and additives such as di(*t*-butyl azodihydrazine) (11). One major drawback with the majority of the systems reported above is the use of environmentally harmful organic solvents such as toluene (12, 14–16), ethylene carbonate (13), trifluoro toluene (17), dichloro methane (18), or chlorobenzene (19), which makes the recovery of products and catalyst difficult. Aerobic oxidation of alcohols using Pd and Pt/C has also occurred but it is limited to water-soluble alcohols (20). Sheldon and co-workers recently reported aerobic oxidation of a variety of alcohols in aqueous phase using a water-soluble palladium(II) bathophenanthroline complex catalyst with high conversion and selectivity (21). Even though the method seems to be attractive, it involves long reaction times (5–15 h) under pressure (3 MPa) as well as expensive and complex catalyst preparation. In addition, most of these methods are carried out at very low concentration levels, which may involve challenging product and catalyst separation steps. Another study reports the oxidation of primary alcohols and α,β -unsaturated alcohols using heterogeneous

¹ To whom correspondence should be addressed. Fax: 513-569-7677. E-mail: Sahle-Demessie.Endalkachew@epa.gov.

FeZSM-5 catalysts and H_2O_2 with high yield and selectivity; however, it involves a high reaction time (20 h) and the use of organic solvents such as methanol (22). A very recent study by Jensen *et al.* reports a method for enantioselective aerobic oxidation of alcohols using a (-)-spartein/Pd(II) complex catalyst (23). The method is good for benzylic alcohols and its application to other substrates is being investigated. This method also requires the presence of an organic solvent and a base. A review of the recent developments in catalytic alcohol oxidation using O_2 and H_2O_2 as primary oxidants has appeared recently (24). In industrial chemistry, heterogeneous catalyst systems have some advantages over homogeneous systems, such as easy recyclability and separability. However, most of the heterogeneous catalyst systems lack good conversion and selectivity. Therefore, an important challenge is to develop active and selective heterogeneous catalyst systems for this type of reaction.

The objective of this study was to conduct selective photooxidation of alcohols on a TiO_2 surface. TiO_2 is biologically and chemically inert and stable with respect to photocorrosion and chemical corrosion and is relatively inexpensive. Titanium dioxide particles absorb light in the wavelength region of 315–380 nm and electron–hole pairs are generated at the particle/solution interfaces (25). The photogenerated hole is believed to have an oxidation potential of ca. 3.0 V and has, therefore, considerable oxidizing capability. In order to intercept the energetically favorable and rapid process of electron–hole recombination, the species to be oxidized is believed to adsorb on the surface of the particles (26). Therefore, photochemical reactions at particle/solution interfaces are controlled by both relative redox energies and adsorption characteristics. The anatase form of TiO_2 has been the most extensively employed in photocatalytic reactions because of its high activity and chemical stability (27–31). The feasibility of this technology on a commercial scale has also been demonstrated by the implementation of numerous small-scale applications, including treatment of air and water streams. Photocatalytic reactions are applicable to a wide range of valuable industrial processes, including organic synthesis, photodestruction of toxic compounds, and purification of drinking water (32, 33). Over the past two decades, there has been considerable work aimed at utilizing semiconductors as photocatalysts (34–43). The photocatalytic oxidation of many organic molecules, including saturated hydrocarbons, by optically excited semiconductor oxides is thermodynamically allowed in the presence of oxygen at room temperature. Selectivities different from those obtained by other oxidation means have been reported (34, 36), showing the potential of the method for syntheses where the expected product is obtained with an acceptable quantum yield. However, the use of this system for the selective oxidation of alcohols has been rather limited. There are few reports that use TiO_2 and metallized TiO_2 as photocata-

lysts for the oxidation of lower alcohols, such as methanol and ethanol (44–46). Chen *et al.* have studied the photocatalytic oxidation of isopropanol using amorphous manganese oxide as the photocatalyst (47). This paper presents a systematic and rigorous study of selective photooxidation of higher alcohols on the TiO_2 surface.

To achieve the desired oxygenates, air/ O_2 and the alcohol are reacted at atmospheric pressure and at temperatures in the range 423–463 K in a photochemical reactor that uses ultraviolet light and immobilized TiO_2 on silica cloth. This work also incorporates the concept of green chemistry and engineering by allowing the production of oxygenates in a selective manner and producing fewer by-products and pollutants than the conventional techniques that use stoichiometric oxidants. TiO_2 is used in the form of a deposited film, since the film photocatalyst system has the following practical benefits not attainable in the powder system: (i) the catalyst filtration step after the reaction is not necessary, and (ii) measurement of the photocatalytic effect can be repeated. Therefore, it is of high technological importance that a TiO_2 film with high photoactivity be prepared.

EXPERIMENTAL

Reagents

All the alcohol substrates as well as titanium isopropoxide were obtained from Aldrich Chemical Company and used as received without any further purification.

Catalyst Preparation by Dip-Coating Method

TiO_2 -coated pads were prepared by the dip-coating method, where preshrunk silica quartz fiber mats (Thermal Material Systems, Brentwood, CA) of dimension $7.6 \times 35 \text{ cm}^2$ were dipped in a saturated solution of neat titanium tetraisopropoxide followed by overnight drying at room temperature (48). During this drying step, the isopropoxide was hydrolyzed by reaction with moisture in the air to form amorphous TiO_2 on the surface. The dry coated fabrics were then calcined in air at 773 K for 3 h, during which time the amorphous titania was converted into the catalytically more active anatase phase. The primary particle size of the TiO_2 film was determined to be about 140 nm (48). These pads were made in the form of hollow cylindrical shapes by wrapping them around a suitable stainless-steel wire mesh.

Reactor Setup

The geometry of the photoreactor has a major effect on this process. A 30-cm-long stainless-steel (304 Grade) annular reactor of 9.7-cm i.d. with an annular volume of 2500 cm^3 was employed. The reactor was fitted with a magnetic stirrer

at the bottom and a cylindrical water-cooled glass jacket containing a 1000-W UV lamp (Jaylight Co., JSZ4378, peak radiation at 360 nm) at the middle. The magnetic stirrer was intended to improve the mixing inside the reactor and to ensure turbulent conditions and uniform contact of the reactants with the catalyst-coated surface. The intensity of the UV light on the catalyst-coated surface was measured approximately (20 mW/cm^2) using a photometer (International Light, Model IL 1400). Three TiO_2 cylindrical pads, prepared as mentioned above, with a total exposed surface area of 765 cm^2 , were fixed on the internal surface of the reactor. Temperatures at the inlet, middle, and bottom of the reactor were measured by three iron–constantan thermocouples. The schematic of the reactor setup is shown in Fig. 1.

Reaction Procedure

Photocatalytic oxidations of alcohols were performed in gas phase using the annular reactor described above by flowing a preheated, humidified air–oxygen mixture and the alcohol vapor. Alcohol was introduced into the reactor system via a metering pump at a particular rate wherein it was heated and vaporized prior to being fed into a static mixer

(Omega FMX 8400). Two mass flow controllers (Kobold MFC-5108) were used to establish the desired flows of air and supplementary oxygen and/or nitrogen. Water vapor was introduced into the flowing air by bubbling it through a water reservoir kept at a controlled temperature. The water-laden air was then passed through a shell and tube heat exchanger kept at 373 K using a high-pressure micrometering plunger pump (Omega PHP-202) followed by mixing with the vaporized alcohol in the static mixer, maintained at 423 K. Excess water was drained from the tubing periodically to avoid entrapment. The preheated mixture was introduced into the bottom of the annular reactor. The flow system was allowed to reach steady state for 60 min with air flowing and the lamp was turned on before introducing the alcohol feed. An average total gas flow rate of 2 L min^{-1} was used with the bottom stirrer at 600 rpm, resulting in a minimal mass transfer resistance, as verified by calculations similar to those of Peral and Ollis (49). The exit stream from the reactor was passed through a liquid nitrogen-cooled trap to condense the oxidized products before being vented to a fume hood.

The condensed liquid products were collected periodically and analyzed by a Hewlett–Packard 6890 gas chromatograph using a HP-5 5% phenyl methyl siloxane

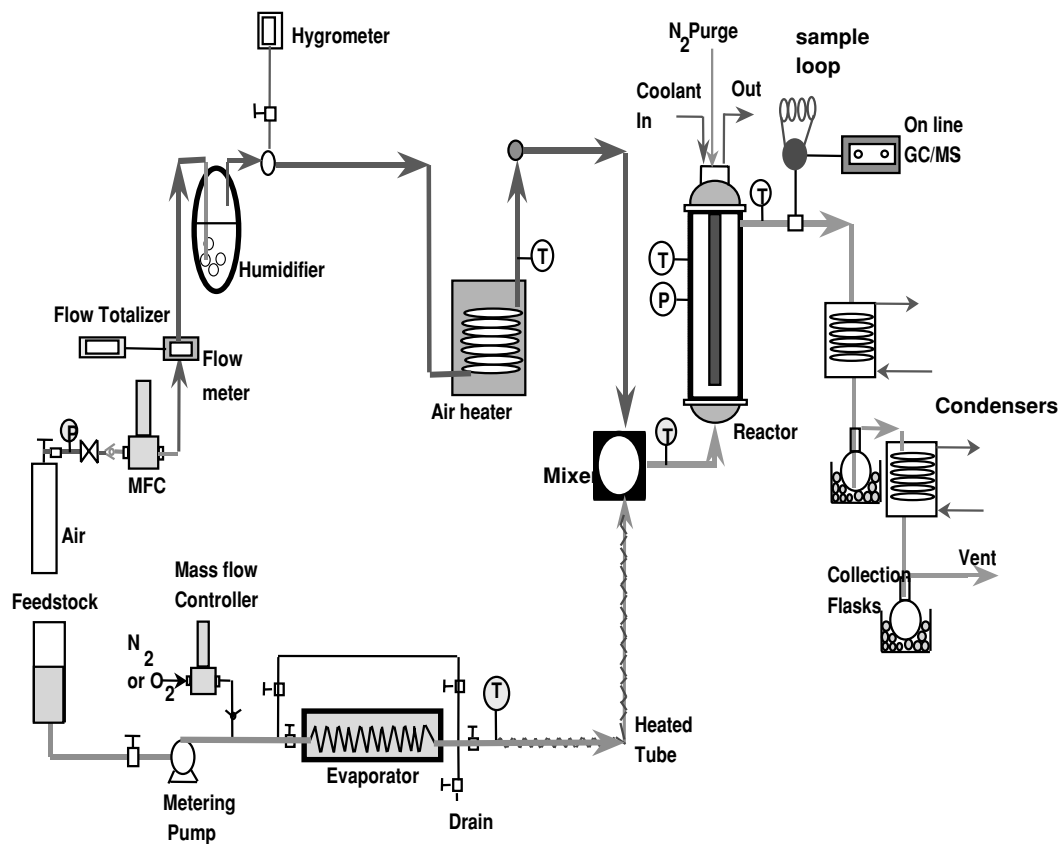


FIG. 1. Schematic diagram of the reactor assembly and experimental setup for the gas-phase photocatalytic oxidation of alcohols.

capillary column (30 m × 320 μm × 0.25 μm) and a quadrupole mass filter-equipped HP 5973 mass selective detector under temperature-programmed heating from 313–473 K at 10°/min. Samples were analyzed with an injection volume of 1 μL. Quantification of the oxygenated products was obtained using a multipoint calibration curve for each product. The presence of any organic acids in the product mixture was determined by HPLC (Finniganmat—LCQ) analysis of the methanol extracts (neutral pH) from the spent catalyst, where the catalyst was scratched off the silica fabric after the reaction and mixed well with methanol (25 mL) followed by filtration. The filtrate was concentrated under vacuum and analyzed.

The alcohol substrates studied include primary, secondary, and cyclic aliphatic and benzylic alcohols. The effects on conversion and product selectivity of different variables, such as O₂/alcohol molar ratio, contact time, water vapor, UV light, and time-on-stream, were investigated. Conversion and selectivity are defined as follows:

$$\text{Conversion (\%)} = \frac{\text{Moles of reactant consumed}}{\text{Initial moles of reactant}} \times 100; \quad [1]$$

$$\begin{aligned} \text{Selectivity of product } P (\%) \\ = \frac{\text{Percentage formation of product } P}{\text{Percentage of total conversion}} \times 100. \end{aligned} \quad [2]$$

TGA Analysis

Catalyst deactivation studies were carried out using thermogravimetric analysis of the fresh TiO₂ and the catalyst after different reaction periods, using a Perkin–Elmer thermogravimetric analyzer (Model TGA-7). Approximately 10 mg of the sample was heated in an atmosphere of air in the temperature range 323–1023 K at a heating rate of 10°/min.

IR Spectroscopy

Catalyst deactivation studies were also conducted by FTIR spectroscopic analysis of benzaldehyde, benzoic acid, acetophenone, and the spent catalyst to identify the potential intermediates formed on the TiO₂ surface during the photocatalytic oxidation of alcohols using a Perkin–Elmer FTIR spectrometer (Model Spectrum 2000). A disposable IR card (3M, Type 61, polyethylene) adsorbed with a methanolic solution of benzaldehyde, benzoic acid, acetophenone, and the methanol extracts from the spent catalysts was used for the analysis and further comparison. The spectral region from 1100 to 2000 cm⁻¹ was analyzed for identification of adsorbed aromatic compounds such as aldehydes and carboxylic acids (50).



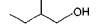
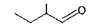
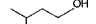
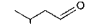






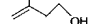



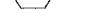
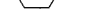
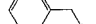
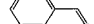
RESULTS

Effect of the Nature of Alcohol

Oxidation results of different alcohols obtained after a reaction period of 2 h are shown in Table 1. This amount of time was chosen to make sure that activity and product selectivity determinations were made at steady-state conditions. All the alcohols except the two phenyl ethanols formed the corresponding carbonyl compound selectively. Generally, the conversions per pass were low for primary alcohols, with a slightly higher value for secondary alcohols. The presence of a benzene ring in the alcohol generally increased the conversion, and the higher the chain length, the greater the conversion. 1-Phenyl ethanol showed the maximum conversion, 97%, among all the alcohols. Oxidation of 3-methyl-3-butene-1-ol yielded 3-methyl-2-butenal and not the expected 3-methyl-3-butene-1-al. This could be due to a double bond migration to the secondary carbon position during the oxidation process. 1-Phenyl ethanol and 2-phenyl ethanol, however, formed mainly the secondary reaction products instead of their primary oxidation carbonyl product. For example, 1-phenyl ethanol gave styrene almost selectively instead of its primary oxidation product, acetophenone. Similarly, 2-phenyl ethanol yielded benzaldehyde as the main product instead of the expected primary oxidation product, phenyl acetaldehyde. Turnover frequencies (TOF) ranging from 7 to 32 × 10⁻³ s⁻¹ were estimated for the alcohols in Table 1 using a surface coverage of 330 micromoles per gram of TiO₂ (45).

TABLE 1

Effect of the Nature of the Alcohol on Conversion and Selectivity^a

| Entry | Alcohol | Product | Conversion ^b (%) | Selectivity (%) |
|-------|---|--|-----------------------------|---|
| 1 |  |  | 18 | >95 |
| 2 |  |  | 20 | >95 |
| 3 |  |  | 24 | >95 |
| 4 |  |  | 26 | >95 |
| 5 |  |  | 37 | >95 |
| 6 |  |  | 14 | >95 |
| 7 |  |  | 21 | >95 |
| 8 |  |  | 35 | >95 |
| 9 |  |  | 97 | 7 (83% styrene) |
| 10 |  |  | 53 | 26 (benzaldehyde = 48, acetophenone = 10) |

^a Alcohol, 1.43 mmol min⁻¹; O₂/alcohol, 22; temperature, 463 K.

^b After a 2-h reaction period.

TABLE 2
Effect of O₂/Alcohol Molar Ratio on 2-Phenyl Ethanol Photocatalytic Oxidation^a

| O ₂ /substrate ratio | Conv. (%) | Selectivity (%) | | | | | | | |
|---------------------------------|-----------|-----------------|---------------------|--------------|---------|-------|---------|---------------|-----------------|
| | | Benzaldehyde | Phenyl acetaldehyde | Acetophenone | Styrene | Ester | Toluene | Ethyl benzene | Propionaldehyde |
| 0 (only N ₂) | 13 | — | 13 | — | — | — | 40 | 22 | 26 |
| 1 | 20 | 36 | 37 | 4 | 2 | 4 | 15 | 2 | — |
| 11 | 36 | 44 | 29 | 7 | — | 10 | 6 | — | — |
| 22 | 53 | 48 | 26 | 10 | 2 | 6 | 7 | — | 1 |
| 34 | 49 | 49 | 18 | 9 | 3 | 9 | 8 | — | 4 |
| 45 | 51 | 51 | 18 | 8 | 2 | 11 | 6 | 1 | 1 |
| 56 | 53 | 43 | 19 | 5 | — | 16 | 14 | 2 | — |

^a Alcohol, 1.43 mmol min⁻¹; temperature, 463 K.

Since all the alcohols except the phenyl ethanols formed only the corresponding carbonyl product selectively, 2-phenyl ethanol was selected for investigating the effects of various reaction parameters, as described below.

Effect of Oxygen-to-Alcohol Molar Ratio

The effect of the oxygen-to-alcohol molar ratio on conversion and product selectivity for the gas-phase photocatalytic oxidation of 2-phenyl ethanol is shown in Table 2. Conversion increased from 13 to 20% when a very small quantity of oxygen (O₂/alcohol = 1) was added to the nitrogen carrier gas. There was significant improvement in the conversion, from 13 to 36%, when nitrogen was replaced by air as the carrier gas (O₂/alcohol = 11). As the oxygen content increased further, conversion also increased, reaching a plateau at an oxygen-to-alcohol molar ratio of 22. Table 2 also shows the effect of the oxygen-to-alcohol molar ratio on product selectivity. In the absence of oxygen, the main products were toluene and ethyl benzene, and no appreciable aldehyde formation was observed. When air was used instead of nitrogen (O₂/alcohol = 11), the main products were aldehydes, and there was hardly any hydrocarbon formation. However, there was no significant change in the product distribution with a further increase in the concentration of oxygen in the feed. These results show that the presence of oxygen is very critical for obtaining a

good conversion and aldehyde formation. A large excess of oxygen (O₂/alcohol ≥ 22) does not have any significant effect on the formation of products. No overoxidation products, such as acid formation, were detected in any case. This was confirmed by HPLC analysis of the methanol extracts from the spent catalyst.

Effect of Gas Flow Rate (Contact Time)

Effect of contact time of the reactant was studied by varying the gas flow at a constant oxygen-to-reactant molar ratio of 22 (Table 3). Conversion increased from 17 to 60% as the total gas flow decreased from 4 to 0.8 L min⁻¹ (contact time increased from 16 to 80 s). Benzaldehyde selectivity increased from 30 to 69%, whereas selectivity for phenyl acetaldehyde decreased from 40 to 20% in the same flow-range variation. Acetophenone was not formed significantly under these conditions and hence its selectivity variation was not important.

Effect of UV Light

The significant role of UV light on the reaction is shown in Fig. 2. When the reactor was heated to 423 K by an external heating source, only 8% conversion was obtained. Irradiation of the catalyst with the UV light increased the conversion dramatically, to 48%. However, the selectivity of phenyl acetaldehyde decreased from 80 to 22% when

TABLE 3
Effect of Total Gas Flow (Contact Time) on 2-Phenyl Ethanol Photocatalytic Oxidation^a

| Total gas flow (L min ⁻¹) | Contact time (s) | Conversion (%) | Selectivity (%) | | |
|---------------------------------------|------------------|----------------|-----------------|---------------------|--------------|
| | | | Benzaldehyde | Phenyl acetaldehyde | Acetophenone |
| 4 | 16 | 17 | 30 | 40 | — |
| 2 | 32 | 53 | 48 | 26 | 10 |
| 1.2 | 53 | 57 | 62 | 23 | 12 |
| 0.8 | 80 | 60 | 69 | 22 | 8 |

^a Alcohol, 1.43 mmol min⁻¹; temperature, 463 K; O₂/alcohol molar ratio, 22.

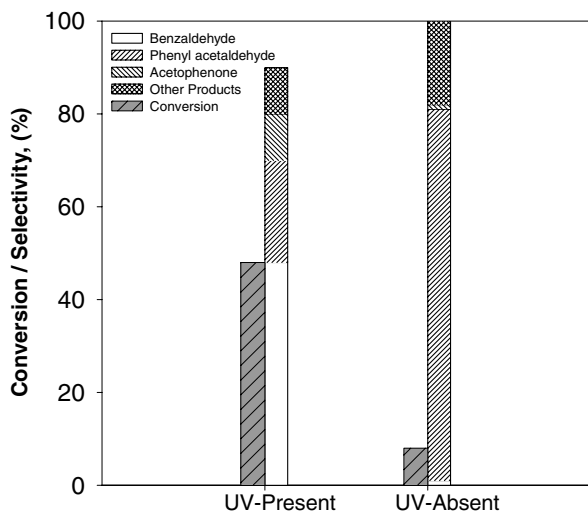


FIG. 2. Effect of UV light on the activity and selectivity of 2-phenyl ethanol oxidation (temperature, 423 K; O_2 /alcohol molar ratio, 22; alcohol, $1.43 \text{ mmol min}^{-1}$).

UV light was used at the same temperature. In the presence of UV light, benzaldehyde was formed in preference to phenyl acetaldehyde, in addition to small amounts of other secondary and tertiary reaction products.

Effect of Water Vapor

The presence of humidity in the feed is also shown to affect the reaction (Fig. 3). When the carrier gas was enriched with water vapor (relative humidity of 90%), conversion remained more or less the same but there was an increased yield of aldehydes. In the absence of water vapor in the feed, appreciable amounts of other secondary and tertiary prod-

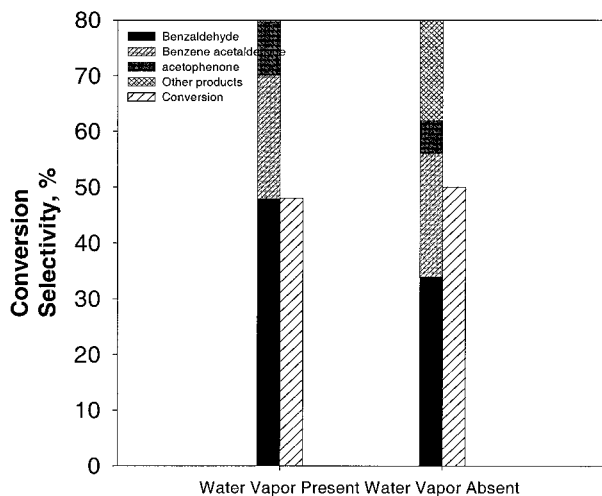


FIG. 3. Effect of water vapor on the activity and selectivity of 2-phenyl ethanol oxidation (temperature, 423 K; O_2 /alcohol molar ratio, 22; alcohol, $1.43 \text{ mmol min}^{-1}$).

ucts, such as ethyl benzene and esters, were also formed. Humidity is known to play a key role in hydrocarbon oxidations through the formation of hydroxyl groups on the catalyst surface (51). However, it does not seem to have any dramatic effect on alcohol oxidation.

Catalyst Deactivation: Effect of Time-on-Stream

Effect of time-on-stream on alcohol conversion is shown in Table 4. Generally, conversion decreases with an increase in time-on-stream for all alcohols studied. This is attributed to the deactivation of the catalyst, which is very common in this type of reaction (52–54). However, the magnitude of the decrease was related to the conversion value and the nature of the alcohol or the products formed. The decrease was less pronounced in the case of alcohols that show low conversions. The higher the conversion, the greater the extent of deactivation, except in the case of 1-phenyl ethanol, which did not show any significant deactivation during the period studied. For example, there was about a 10–30% reduction in conversion for C5 alcohols, whereas C6 alcohols such as cyclohexanol, benzyl alcohol, and 2-phenyl ethanol showed around a 65% reduction in conversion as the reaction period increased from 1 to 4 h. The selectivity for the corresponding carbonyl compound was almost 100% for all the aliphatic alcohols irrespective of the extent of conversion. However, the product distribution varied with reaction time for 1-phenyl and 2-phenyl ethanol oxidations (Figs. 4a and 4b). It can be seen that the product composition consisted of a significant amount of acetophenone in both cases during the initial period (1 h). As the reaction period increased, acetophenone selectivity decreased drastically and formation of other products ensued. The catalyst after the reaction was extracted with methanol and analyzed by HPLC for the possible formation of overoxidation products, such as acids. The analysis

TABLE 4
Effect of Time-on-Stream on Conversion and Selectivity of Various Alcohols^a

| Alcohol | Conversion (%) at different reaction times | | |
|------------------------|--|-----|-----|
| | 1 h | 2 h | 4 h |
| 1-Pentanol | 26 | 20 | 17 |
| 2-Pentanol | 19 | 18 | 17 |
| 3-Pentanol | 34 | 24 | 21 |
| Cyclopentanol | 48 | 37 | 24 |
| Hexyl alcohol | 45 | 26 | 21 |
| Cyclohexanol | 38 | 21 | 14 |
| 3-Methyl-3-butene-1-ol | 25 | 14 | 04 |
| Benzyl alcohol | 52 | 35 | 18 |
| 1-Phenyl ethanol | 90 | 97 | 94 |
| 2-Phenyl ethanol | 64 | 53 | 20 |

^a Alcohol, $1.43 \text{ mmol min}^{-1}$; temperature, 463 K; O_2 /alcohol molar ratio, 22.

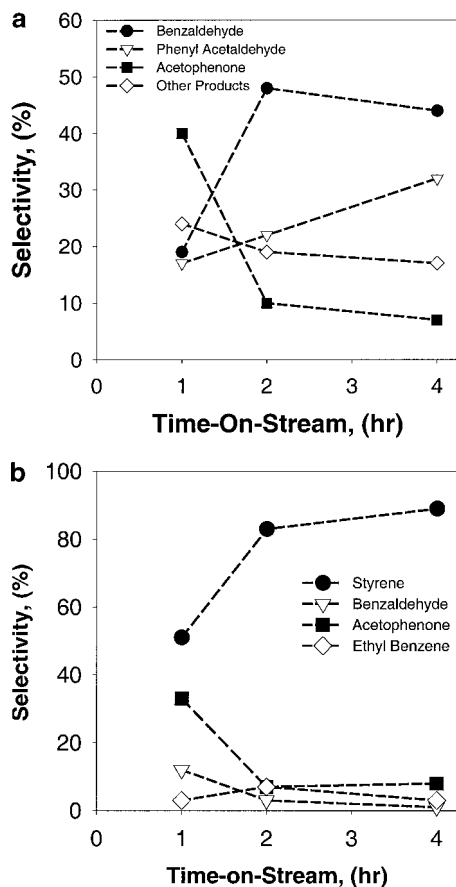


FIG. 4. (a) Effect of reaction run time on product selectivity for 1-phenyl ethanol photooxidation. (b) Effect of reaction run time on product selectivity for 2-phenyl ethanol photooxidation (temperature, 423 K; O_2 /alcohol molar ratio, 22; alcohol, $1.43 \text{ mmol min}^{-1}$).

showed the presence of the initial reactant and products such as benzaldehyde and phenyl acetaldehyde as well as some carboxylate-type compound on the surface. No detectable acids could be identified. However, the methanol extraction did not remove all the carbon compounds from the catalyst, as evidenced by the dark color of the catalyst even after methanol washing. The catalyst surface after the extended reaction period (4 h) was slightly sticky, with a yellowish-brown appearance.

Thermogravimetric Analysis

Thermogravimetric analysis (TGA) of the fresh catalyst and the catalysts after different reaction periods showed a broad thermogram with a slow rate of weight loss in the temperature range 373–973 K (Fig. 5). The values of percentage weight loss and temperature of the onset of weight loss are given in Table 5. Weight loss is a measure of the amount of product adsorbed on the catalyst surface. The catalyst after 1 h of reaction showed a gross weight loss of 2.6%, in comparison to 0.8% loss for the fresh catalyst.

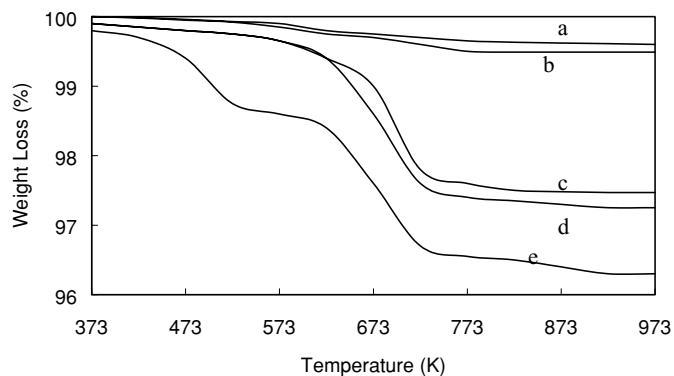


FIG. 5. Thermograms of the fresh and used catalysts. (a) Fresh catalyst; (b) regenerated catalyst; (c) catalyst after a 1-h reaction period; (d) catalyst after a 2-h reaction period; and (e) catalyst after a 4-h reaction period.

An increase in the reaction time to 2 and 4 h increased the weight loss to 3 and 3.7%, respectively. The onset of weight loss was around 650 K, followed by a slow and steady decrease up to around 773 K. The catalyst after 4 h of reaction, however, showed a two-step weight loss process, with the initial weight loss occurring at around 473 K and the second one at the same temperature as that of the other two catalysts. The figure also shows that calcining in air at 773 K for 3 h could regenerate the catalyst, almost completely, to its original form.

IR Spectroscopic Analysis

IR spectra from the spent catalyst sample is shown in Fig. 6 along with the spectra for benzaldehyde, benzoic acid, and acetophenone for identification of the surface species present on the catalyst surface which is believed to be responsible for the deactivation. A comparison of the spectra suggests that the spent catalyst surface contains aromatic and aldehydic species. The IR spectrum of the spent catalyst also indicates the presence of some polymeric carboxylate compound. No indication of any acid formation could be observed. This is in agreement with both the HPLC analysis and the TGA experiments, as discussed above.

TABLE 5
Thermogravimetric Analysis Data of the Fresh and Used Catalyst

| Reaction time of the catalyst (h) | Onset of weight loss (K) | Weight loss (%) |
|-----------------------------------|--------------------------|-----------------|
| 0 (fresh) | — | 0.8 |
| 1 | 652 | 2.6 |
| 2 | 649 | 3.0 |
| 4 | 648 | 3.7 |
| Regenerated | — | 1.0 |

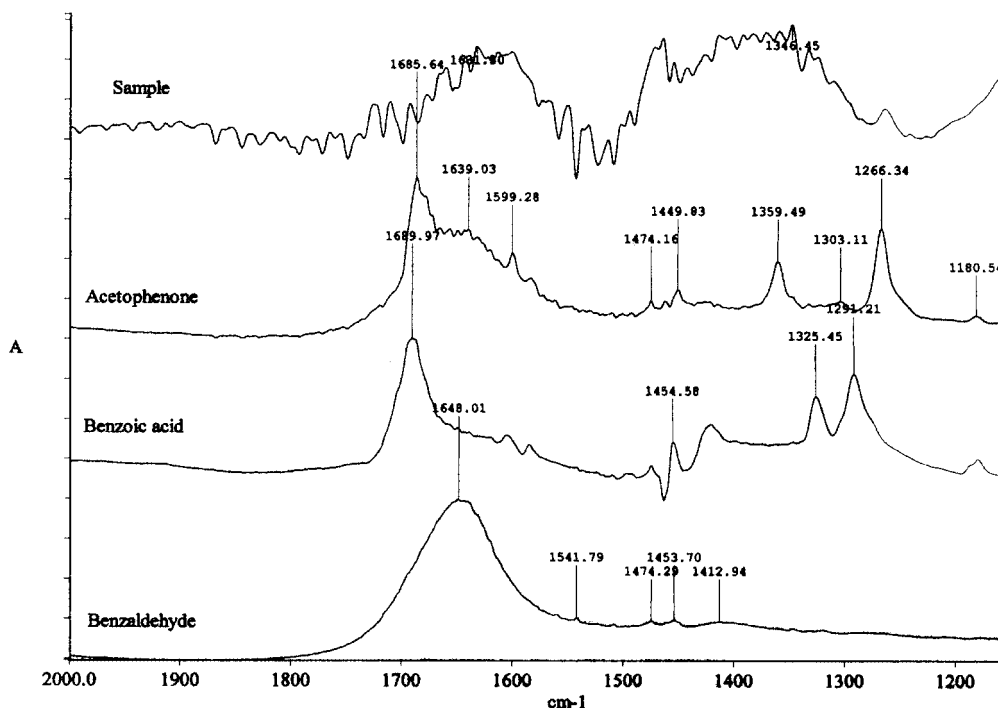


FIG. 6. FTIR spectra of adsorbed methanolic solutions of spent catalyst sample, acetophenone, benzoic acid, and benzaldehyde.

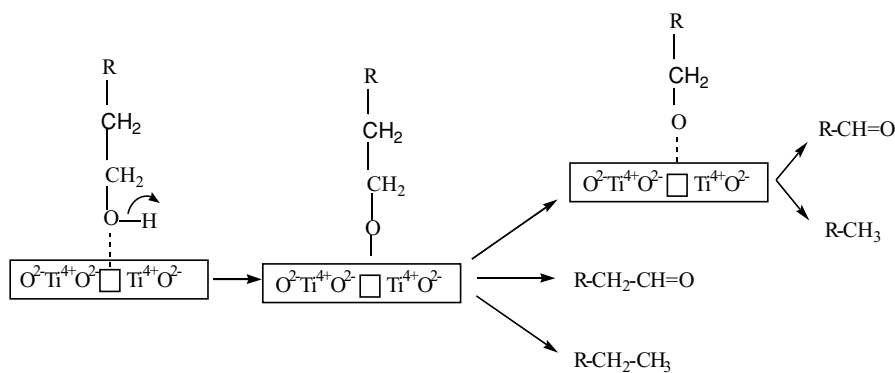
DISCUSSION

Effect of the Nature of Alcohol on Conversion and Selectivity

Activity for photocatalytic oxidation of alcohols is found to be very much dependent on the nature of the alcohol used. During photocatalytic oxidation, the initial reaction of the alcohol takes place on the surface of TiO_2 where the primary hole reaches the surface and interacts with the surface hydroxyl groups, followed by an electron transfer to the hole to form species such as OH^\cdot and $\equiv\text{TiO}^\cdot$ (55). These species react via a mediated pathway. At high alcohol concentration, as is the case here, there could also be a direct interaction of the surface hole with the hydroxyl group of

the alcohol (56). In addition, the alcohols may undergo dehydration on the catalyst surface during a photocatalytic oxidation reaction (57).

The initial photooxidation step here may be the interaction of a surface hole with the hydroxyl group of the alcohol forming a metal-oxo species with the removal of a proton (Scheme 1). This proton removal step becomes easier with an increase in carbon chain branching as well as with an increase in carbon chain length, because of the increased availability of adjacent removable protons. The higher the number of adjacent hydrogen atoms present, the easier the removal and the greater the conversion. Temperature also plays a role here; therefore, this effect may not be pronounced at higher temperature. The nature of the alkyl



SCHEME 1. Photocatalytic oxidation of alcohols to aldehyde/ketone over TiO_2 (\square = surface hole).

group also influences the above step, as is evident from Table 1. Cyclopentanol (entry 5) showed a higher conversion than its open-chain counterparts, viz. 2- and 3-pentanol (entries 2 and 3). This could be due to the higher strain in the 5-carbon cyclic structure. However, cyclohexanol (entry 7) gave a lower conversion than *n*-hexanol (entry 4) due to the increased stability of the six-carbon cyclic structure (58). It was also observed that the presence of a benzene ring enhanced the conversion (entries 8–10). This can be attributed to the electron-deficient nature of the benzene ring, which results in a reduced electron density at the oxygen–hydrogen bond, thereby making the proton abstraction relatively easy. Formation of styrene from 1-phenyl ethanol (entry 9) may be due to the photocatalytic-induced dehydration of the alcohol (57).

Two types of adsorption sites are present on TiO₂ during photocatalytic oxidation (45): a weakly adsorbed site, where the carbonyl product formed readily gets desorbed, and a strongly adsorbed site, where the primary product undergoes further reactions to form other secondary and tertiary oxidation products, as may be case for 2-phenyl ethanol (Scheme 1).

Effect of Oxygen-to-Substrate Ratio

The presence of oxygen is necessary for photocatalytic oxidation to take place (Table 2). The effect of oxygen concentration, however, diminishes at high oxygen levels ($O_2/\text{alcohol} \geq 22$). Molecular oxygen is activated on the catalyst surface in the presence of UV light to form electrophilic species such as O^{2-} and O^- , which also helps in activating the reactant molecule and eventually in producing different oxidation products. When no oxygen is available, the holes formed on the surface on UV irradiation abstract the oxygen from the alcohol, producing hydrocarbons such as toluene and ethyl benzene, as illustrated in Scheme 1. Anaerobic conditions can result in photocatalytic-assisted hydrolysis reaction (57a). It is also obvious from the scheme that a large excess of oxygen has no additional benefits. Boarini *et al.* have made a similar observation in the photocatalytic oxidation of cyclohexane (43).

Effect of Gas Flow Rate (Contact Time)

The effect of residence time studied using the photocatalytic oxidation of 2-phenyl ethanol shows that an increase in the residence time of the alcohol in the reactor facilitates the formation of secondary products such as benzaldehyde at the cost of the primary oxidation product, phenyl acetaldehyde (Table 3). In other words, a high residence time of the molecule in the reactor means the intermediate products can adsorb and react further down the reactor to form more strongly bound products that cause catalyst deactivation (45).

Effect of UV Light

UV light is required for the activation of the catalyst surface as well as the molecular oxygen (Fig. 2). Heating the catalyst to the same temperature by an external source may not produce the same type of active sites on the surface as is produced by UV irradiation. In other words, the photocatalytic sites could be completely different from the thermal reaction sites. It may be assumed that the UV irradiation of the catalyst surface results in photocatalytically active sites, which are stronger oxidants than the sites produced by the thermal effect, which causes only mild oxidation. This mild oxidation affords mainly the primary oxidation product, whereas strong oxidation affords more secondary products. This explains why phenyl acetaldehyde is selectively formed in the absence of UV light whereas benzaldehyde is the main product in the presence of UV light. Both the UV and thermal effect may be operating in parallel during the photocatalytic oxidation (45c), even though the thermal effect is not the predominant one determining the overall activity and product selectivity. An increase in light intensity accelerates the reaction; however, the increase in photoactivity is not linear with the light intensity (59, 60).

Effect of Water Vapor

Results show that humidity in the feed affects the alcohol oxidation (Fig. 3). However, the role of humidity in photocatalytic oxidation of alcohols is not very critical. Water vapor is known to contribute to the formation of surface hydroxyl groups by coordination with surface holes. The presence of surface hydroxyl groups is necessary for the oxidation process. In the absence of water vapor in the feed, the degree of surface hydroxylation is less. This reduces the formation of oxidation products (aldehydes) and enhances dehydration products such as alkanes and alkenes. Exposure of the catalyst to UV light under dry conditions leads to irreversible consumption of the surface hydroxyl groups, which in turn results in catalyst deactivation (61). In alcohol oxidation, this surface hydroxylation can be partly achieved by the alcohol itself.

Catalyst Deactivation: Time-on-Stream, TGA, and IR Studies

The decrease in conversion with reaction pass time is attributed to the deactivation of the catalyst surface, as mentioned earlier. The product selectivity for the two phenyl ethanols also varies with time-on-stream (Fig. 4). Acetophenone is observed as the main product during the initial reaction period, indicating that it is one of the primary products of oxidation formed from the weakly adsorbed sites. With an increase in reaction pass time, more and more strongly adsorbed species are formed, leading to the formation of secondary oxidation products, such as aldehydes (45).

TGA analysis of the fresh TiO_2 and the TiO_2 after different reaction periods indicates that catalyst deactivation occurs in the first hour of the reaction itself. The initial rate of the reaction is higher than at steady state for almost all the alcohols tested. This initial deactivation may be due to the accumulation of the product on the catalyst surface (45b). Most of the weight loss occurs at around 650 K, indicating the presence of a carbonaceous deposit on its surface. However, the broad thermogram indicates that it is not just simple carbon but some carboxylate compound. The concentrations of both the reactant and the carboxylate-type material increase with an increase in the reaction period. The yellowish-brown appearance with a slightly sticky nature of the spent catalyst surface indicates the presence of some polymeric material formed by the polymerization of the aldehyde products. The longer the reaction period, the greater its formation. Similar oligomerization was detected during the gas-phase photocatalytic oxidation of acetaldehyde on the TiO_2 surface (45d). The appearance of an additional peak at 473 K in the thermogram may be due to this reason. The fact that a 3-h calcination of the catalyst in air at 773 K regenerates the catalyst almost completely also suggests that it is mostly carbonaceous material that deactivates the catalyst. HPLC analysis of the methanol extracts from the catalyst surface after the reaction also confirmed the presence of some carboxylate-type compounds on the surface. This is further confirmed by the IR analysis of the spent catalyst, which also shows the presence of some aldehydic and polymeric species.

Catalyst deactivation during photocatalytic reactions have been observed by many workers (52–54, 62, 63). Many hypotheses have been used to explain the catalyst deactivation during photooxidation. For example, Falconer and co-workers identified the accumulation of acetaldehyde on the catalyst surface for the deactivation of the catalyst during the photocatalytic oxidation of ethanol (45). Peral and Ollis proposed that strongly adsorbed 1-butanoic acid causes catalyst deactivation during the photocatalytic oxidation of 1-butanol (49). Cunningham and Hodnett suggested that the deactivation is caused by the adsorption of CO_2 formed during the reaction on the active sites (62). Blake and Griffin observed carboxylate-type species accumulating on the catalyst surface during butanol oxidation (64). Strongly adsorbed carbonate species are reported to cause catalyst deactivation during the photooxidation of trichloroethylene (65). Ollis and co-workers have also reported that carboxylate and carboxylic acid accumulation are responsible for deactivation during the photooxidation of toluene and toluene mixed with trichloroethylene, trichloropropene, or perchloroethylene (66, 67).

The relative photonic efficiencies for the initial oxidation of the organic substrates in the gas-phase reactor using a TiO_2 film are estimated to be in the range 0.8–1.2. The estimated quantum yields ranged from 0.005 to 0.02 (68). The “electrical energy per order” (EE/O), defined as the

electrical energy needed to change the feed substrate concentration by an order of magnitude, is estimated to be 16 to 18. However, the estimated electrical energy per mass of desired product formed for the photooxidation method is within the order of magnitude of that of the conventional process.

CONCLUSIONS

In summary, UV light-assisted photocatalytic oxidation is found to be suitable for selectively oxidizing primary and secondary aliphatic alcohols to their corresponding carbonyl products using a 2.5-L annular photoreactor containing immobilized TiO_2 catalyst. Aromatic alcohols, however, form mainly secondary reaction products. Oxygen availability is found to be critical for the photooxidation. The presence of water vapor in the feed is advantageous for the reaction; however, it is not as significant as in the case of hydrocarbon oxidation, where its presence is especially important in sustaining the catalyst life (59). One disadvantage of the system is the catalyst deactivation, which is attributed to the surface accumulation of reaction products. The catalyst activity, however, can be regained by calcining the catalyst in air at 723 K for approximately 3 h. The reaction mechanism is described to explain the behavior of the catalyst under different conditions. Conversion and product distribution obtained are explained on the basis of different oxidation mechanisms. The oxidation of alcohols using light-activated TiO_2 catalyst and molecular oxygen could be a green alternative, but further investigation into process development is required.

ACKNOWLEDGMENTS

The authors are grateful to the referees for their critical assessment and valuable suggestions for improving the clarity and quality of the paper. The technical assistance and support in conducting the reaction studies by Mr. Tom Deinlein is gratefully acknowledged. U.R. Pillai is a postgraduate research participant at the National Risk Management Research Laboratory administered by the Oak Ridge Institute for Science and Education through an interagency agreement between the U.S. Department of Energy and the U.S. Environmental Protection Agency.

REFERENCES

1. Sheldon, R. A., and Kochi, J. K., “Metal-Catalyzed Oxidation of Organic Compounds.” Academic Press, New York, 1981.
2. Hudlicky, M., “Oxidations in Organic Chemistry.” Am. Chem. Soc., Washington, DC, 1990.
3. Larock, R. C., “Comprehensive Organic Transformations.” VCH, New York, 1989.
4. Cainelli, G., and Cardillo, G., “Chromium Oxidations in Organic Chemistry.” Springer, Berlin, 1984.
5. Murahashi, S. I., Naota, T., and Hirari, J., *J. Org. Chem.* **58**, 7328 (1993).
6. Inokuchi, T., Nakagawa, K., and Torii, S., *Tetrahedron Letters* **36**, 3223 (1995).
7. Iwahama, T., Sakaguchi, S., Nishiyama, Y., and Ishii, Y., *Tetrahedron Lett.* **36**, 6923 (1995).

8. Capdevielle, P., Sparfel, D., Baranne-Lafont, J., Cuong, N. K., and Maumy, M., *J. Chem. Res.* **10**, 1993 (1993).
9. Munakata, M., Nishibayashi, S., and Sakamoto, H., *J. Chem. Soc. Chem. Commun.* 219 (1980).
10. Senmelhack, M. F., Schmid, C. R., Cortes, D. A., and Chon, C. S., *J. Am. Chem. Soc.* **106**, 3374 (1984).
11. Marko, I. E., Giles, P. R., Tsukazaki, M., Brown, S. M., and Urch, C. J., *Science* **274**, 2044 (1996).
12. Nishimura, T., Onoue, T., Ohe, K., and Uemura, S., *J. Org. Chem.* **64**, 6750 (1999).
13. Blackburn, T. F., and Schwartz, J., *J. Chem. Soc. Chem. Commun.* 157 (1977).
14. Bilgrien, C., Davis, S., and Drago, R. S., *J. Am. Chem. Soc.* **109**, 3786 (1987).
15. Tang, R., Diamond, S. E., Neary, N., and Mares, F., *J. Chem. Soc. Chem. Commun.* 562 (1978).
16. Marko, I. E., Giles, P. R., Tsukazaki, M., Chelle-Regnaut, I., Urch, C. J., and Brown, S. M., *J. Am. Chem. Soc.* **119**, 12661 (1997).
17. Hanyu, A., Takeyawa, E., Sakaguchi, S., and Ishii, Y., *Tetrahedron Lett.* **39**, 5557 (1998).
18. Lenz, R., and Ley, S. V., *J. Chem. Soc. Perkin Trans.* **1**, 3291 (1997).
19. Dijkman, A., Arends, I. W. C. E., and Sheldon, R. A., *Chem. Commun.* 1591 (1999).
20. Mallat, T., and Baiker, A., *Catal. Today* **19**, 247 (1994).
21. Brink, G., Arends, I. W. C. E., and Sheldon, R. A., *Science* **287**, 1636 (2000).
22. Srinivas, N., Radha Rani, V., Radha Kishan, M., Kulkarni, S. J., and Raghavan, K. V., *J. Mol. Catal. A* **172**, 187 (2001).
23. Jensen, D. R., Pugsley, J. S., and Signam, M. S., *J. Am. Chem. Soc.* **123**, 7475 (2001).
24. Sheldon, R. A., Arends, I. W. C. E., and Dijkman, A., *Catal. Today* **57**, 157 (2000).
25. Gerisher, H., and Willig, F., *Top. Curr. Chem.* **61**, 50 (1976).
26. Arbour, C., Sharma, D. K., and Langford, C. H., *J. Chem. Soc. Chem. Commun.* 917 (1987).
27. Matthew, R. W., *J. Catal.* **111**, 264 (1988).
28. Tunesi, S., and Anderson, M. A., *J. Phys. Chem.* **95**, 3399 (1991).
29. Sabate, J., Anderson, M. A., Kikkawa, H., Xu, Q., Cervera-March, S., and Hill, C. G., *J. Catal.* **134**, 36 (1992).
30. Wold, A., *Chem. Mater.* **5**, 280 (1993).
31. Vinodgopal, K., Hotchandani, S., and Kamat, P. V., *J. Phys. Chem.* **97**, 9040 (1993).
32. Al-Ekabi, H., and Serpone, N., *J. Phys. Chem.* **92**, 5726 (1988), and references therein.
33. Matthews, R. W., *J. Phys. Chem.* **91**, 3328 (1987).
34. Fox, M. A., *Acc. Chem. Res.* **16**, 314 (1983).
35. Fox, M. A., *New J. Chem.* **11**, 129 (1987).
36. Ollis, D. F., Hsiao, C. Y., Budiman, L., and Lee, C. L., *J. Catal.* **88**, 89 (1984).
37. Forments, M., Juillet, F., Meriaudeau, P., and Teichner, S. J., *CHEMTECH* **680** (1971).
38. Fox, M. A., and Chen, C. C., *J. Am. Chem. Soc.* **103**, 6757 (1981).
39. Pincock, J. A., Alexandra, L. P., and Fox, M. A., *Tetrahedron* **41**, 4107 (1985).
40. Fox, M. A., *Photocatal. Environ.* **237**, 445 (1988).
41. Worsley, D., Andrew, M., Keith, S., and Hutchings, M. G., *J. Chem. Soc. Chem. Commun.* 1119 (1995).
42. Mao, Y., and Bakac, A., *Inorg. Chem.* **35**, 3925 (1996).
43. Boarini, P., Carassiti, V., Maldotti, A., and Amadelli, A., *Langmuir* **14**, 2080 (1998).
44. Chen, J., Ollis, D. F., Rulkens, W. H., and Bruning, H., *Water Res.* **33**, 661 (1999).
45. (a) Muggli, D. S., McCue, J. T., and Falconer, J. L., *J. Catal.* **173**, 483 (1998); (b) Muggli, D. S., and Falconer, J. L., *J. Catal.* **175**, 213 (1998); (c) Falconer, J. L., and Magrini-Bair, K. A., *J. Catal.* **179**, 171 (1998); (d) Muggli, D. S., Lowery, K. H., and Falconer, J. L., *J. Catal.* **180**, 111 (1998).
46. Hussein, F. H., Pattenden, G., Rudham, R., and Russell, J. J., *Tetrahedron Lett.* **25**, 3363 (1984).
47. Chen, J., Lin, J. C., Purohit, V., Cutlip, M. B., and Suib, S. L., *Catal. Today* **33**, 205 (1997).
48. Sahle-Demessie, E., Gonzalez, M., Wang, Z. M., and Biswas, P., *Ind. Eng. Chem. Res.* **38**, 3276 (1999).
49. Peral, J., and Ollis, D. F., *J. Catal.* **136**, 554 (1992).
50. Socrates, G., "Infrared Characteristic Group Frequencies." Wiley, New York, 1980.
51. Lin, M. M., *Appl. Catal. A* **207**, 1 (2001).
52. Sauer, M. L., and Ollis, D. F., *J. Catal.* **163**, 215 (1996).
53. Colon, G., Hidalgo, M. C., and Navio, J. A., *J. Photochem. Photobiol. A* **138**, 79 (2001).
54. Mendez-Roman, R., and Cardone-Martinez, N., *Catal. Today* **40**, 353 (1998).
55. Minero, C., Mariella, G., Maurino, V., Vione, D., and Pelizzetti, E., *Langmuir* **16**, 8964 (2000).
56. Brezova, V., Vodny, S., Vesely, M., Ceppan, M., and Lapcile, L., *J. Photochem. Photobiol. A* **56**, 125 (1991).
57. (a) Calza, P., Minero, C., and Pelizzetti, E., *Environ. Sci. Technol.* **31**, 2198 (1997); (b) Djeghri, N., and Teichner, S. J., *J. Catal.* **62**, 99 (1980).
58. Smith, M. B., and March, J., in "March's Advanced Organic Chemistry: Reactions, Mechanisms and Structure," 5th ed., p. 180. Wiley-Interscience, New York, 2001.
59. Peterson, M. W., Jurner, J. A., and Nozik, A. J., *J. Phys. Chem.* **95**, 221 (1991).
60. Mills, A., Davies, R. H., and Worsely, D., *Chem. Soc. Rev.* **22**, 417 (1993).
61. Martra, G., Coluccia, S., Marchese, L., Augugliaro, V., and Loddo, V., *Catal. Today* **53**, 353 (1998).
62. Cunningham, J., and Hodnett, B. K., *J. Chem. Soc. Faraday Trans.* **77**, 2777 (1981).
63. Peral, J., and Ollis, D. F., in "Proc. Ist Int. Conf. TiO₂ Photocatalytic Purification and Treatment of Water and Air" (D. F. Ollis and H. Al-Ekabi, Eds.), p. 741. Elsevier, Amsterdam/New York, 1993.
64. Blake, N. R., and Griffin, G. L., *J. Phys. Chem.* **92**, 5697 (1988).
65. Larson, S. A., and Falconer, J. L., *Appl. Catal. B* **4**, 325 (1994).
66. Sauer, M. L., Hale, M. A., and Ollis, D. F., *Photochem. Photobiol. A* **88**, 169 (1995).
67. Luo, Y., and Ollis, D. F., *J. Catal.* **163**, 1 (1996).
68. Serpone, N., *J. Photochem. Photobiol. A* **104**, 1 (1997).